Supplementary Discussion:

The ACE2 program presents several testable hypotheses for studying the cytopathology of infection and the influence of commonly used diabetes and hypertension drugs. For example, ACE2+ signature genes that are also reported to change expression in response to SARS-CoV-2 infection (highlighted in Figure 4C and listed in Supplementary Table 6 “Bojkova proteomes[S1] List”) may directly interface with a SARS-CoV-2 infection in kidney PTEC. To understand the processes impacted by these genes and develop hypotheses for experimental exploration, we clustered the PTEC functional network with this overlap gene list and identified enriched pathways (Supplementary Table 16). Genes involved in endocytosis and endomembrane transport (DNAJC13, CHMP3, SNX9, PDCD6IP) and membrane organization (GOLGA4, ANXA2, ANK3) could facilitate viral entry, replication and exit[S2], and proteins that interact with viral gene transcription (DHX9, HDAC1, NUCKS1, SMARCA4, SMARCB1, CHD1, and RSF1), viral RNA translation (EIF3A, MCTS1, SSB, and DHX9) and viral genome replication (DDX3X, PPIE, and PABPC1) could promote productive replication. Inflammation and interferon response genes included in this overlap gene set include IFNGR1, ILF3, TNFAIP2, TNFAIP8, and successful host defense of SARS-CoV-2 may hinge on their activity. It is intriguing that a number of the ACE2+ DKD signature genes encode for proteins that interact or have been predicted to interact with SARS-CoV-2 proteins[S1], and are involved in anti-host defense response; including the membrane “M” protein (suppresses type 1 interferon responses and modulate cytokine responses)[S3, S4], the nucleoprotein “N” (inhibits autophagy and apoptosis of infected cells through mTOR)[S5], Orf3a (may modulate IL-1B)[S6,S7], and Nsp6 (inhibits phagosome expansion and targeting of viral products to lysosome)[S8]. If these physical interactions occur during the course of SARS-CoV-2 infection and involve negative functional regulation of host-

defense proteins, ACE2+ PTEC could be impaired in their ability to mount an appropriate host response, providing one explanation of increased susceptibility to SARS-CoV-2.

Given the urgent need for novel therapeutic options, intersecting the ACE2 regulatory networks with the complex landscape of interactions between drugs and the gene signature defined here can help to identify therapeutic targets for further study. We identified ACE2+ co-regulated genes annotated in DrugBank as targets of medications regularly taken by patients with DKD. For example, the insulin receptor (INSR, in M4 in Figure 4A, Supplementary Table 2) and the IGF-1 receptor (IGF1R, in M4 in Figure 4A) are overexpressed in ACE2+ PTEC as is DPP4 (in M7 in Figure 4A), a protease associated with entry of other coronaviruses and a key factor in glucose metabolism, targeted by DPP4 inhibitors already in clinical use.

Human kidney organoids, with ACE2 expression in the correct functional context of tubular cell clusters, are promising models with which to test these hypotheses. They supported ACE2-mediated SARS-CoV-2 infection, and the addition of soluble ACE2 reduced cytotoxicity[S9,S10]. Probing gene expression and physical interactions using gene knock-down, over-expression, or drug treatment regimes in the organoids in conjunction with SARS-CoV-2 infection will provide insight into the mechanisms in operation during infection. Thus, combining the organoid model system with the human interaction maps generated in this study can form an experimental framework for mechanistic studies of the cytopathology of infection and the influence of commonly used drugs.

Supplementary Methods:

Study population

DKD biopsy cohort (DKD)

Between 2013 and 2017, 141 American Indians (39 men, 102 women) from southern Arizona with type 2 diabetes were enrolled in an observational study of DKD that included annual research examinations. Glomerular filtration rate (GFR) was measured at each of these examinations by the urinary clearance of iothalamate[S11]. Each participant also underwent a research kidney biopsy used for quantitative morphometry and for compartment-specific tissue expression studies. For kidney biopsies obtained from the last 44 participants enrolled between 2016 and 2017, processing of the kidney specimens was modified to enable scRNAseq studies using kidney biopsy tissues. These 44 participants (DKD) were included in the present study.

At each annual research examination, medicines taken by the participants were recorded. Blood pressure (BP) was measured with the participant resting in a seated position, and height and weight were obtained with the participant dressed in light clothing without shoes. Body mass index was defined as weight in kilograms divided by the square of height in meters. Urine and serum creatinine were measured by an enzymatic method. Urinary albumin excretion was assessed by nephelometric immunoassay and expressed as the albumin/creatinine ratio (ACR) in mg/g creatinine. GFR and HbA1c were measured by high performance liquid chromatography. Because of the level of obesity in the participants, absolute GFR (ml/min) was reported, uncorrected for body surface area[S12]. Clinical and demographic features and the antihypertensive medicines taken by the DKD cohort at the time of the kidney biopsy are shown in Table 1. Participants had mean diabetes duration of 12.2 ± 7.5 years, HbA1c of 9.2 ± 2.4 %, iGFR of 159 ± 58 ml/min with one patient GFR <60ml/min, and median ACR of 18 [9-53] mg/g

(25 persons had a normal ACR <30 mg/g, 14 had moderate albuminuria of 30-300 mg/g and 3 had severe albuminuria >300mg/g of ACR at biopsy).

Owing to ethical considerations, privacy protection concerns, and to avoid identifying individual study participants in vulnerable populations, the Institutional Review Board of the National Institute of Diabetes and Digestive and Kidney Diseases has stipulated that individual-level gene expression and genotype data from the American Indian DKD study cannot be made publicly available.

Living donor (LD) biopsies procured from the Allograft kidney transplant surveillance cohort

The University of Michigan has a kidney transplant surveillance program in which biopsies are performed for clinical care at implantation and 3-, 6- and 12-months post transplantation. A subset of patients in this surveillance program participate in the Human Kidney Transplant Transcriptomic Atlas study, which procures additional biopsy cores for research. Tissue samples from these biopsies were used in the present study. Reference healthy tissue 18 LD biopsies were obtained prior to perfusion and before placement in the recipient.
Participant mean age was 45.1 ± 10.2 years, range (30-66), 11 of the 18 donors were female (61%), mean spot urine protein to creatinine ratio at the time of evaluation was 0.08 ± 0.04 g/g with range (0.03-0.20), mean iothalamate GFR was 100.6 ± 16.9 ml/min/1.73 m^2 with range (81-144). Fifteen of 17 donors were white, one of Hispanic descent and one of African ancestry. All donors were nondiabetic and non-hypertensive. Technical replicates were performed on two LD biopsies with 2 and 3 biopsy segments processed in parallel.

COVID-19 cohort (COV)

In response to the COVID-19 pandemic at the University of Michigan Medical Center a protocol to capture urine samples from SARS-CoV-2 patients was established to allow cell and

molecular biology studies of the kidney-related manifestations in COVID-19. Patients are offered participation in the study upon admission to the hospital and throughout their hospital course. 50 ml of a spot random urine sample was procured specifically for the study, immediately transported to the research laboratory on ice and processed for cell and molecular studies and participants are prospectively followed thereafter.

Patients were eligible to participate if they were adults admitted to the hospital with a positive PCR test for SARS-CoV-22 and had symptoms attributable to SARS-CoV-2. Exclusion criteria included a history of ileal conduit, bladder cancer, anuria or if the initial positive SARS-CoV-2 test was more than a month prior to urine collection. Clinical data were abstracted from the participants' charts and summarized in Table 1. Average participant age was 50 (SD of 17.3) and 54% were male. The median time since the first positive COVID-19 test was 11 days and 62% of the participants had AKI by KDIGO serum creatinine criteria. At the time of urine sample collection, 38% of participants had a down-trending serum creatinine and 85% required ICU admission at some point during their hospitalization. 54% of the participants had diabetes mellitus (DM).

Kidney biopsy sample processing for single cell

Biopsy tissue samples were quickly thawed, washed with culture medium and dissociated to single cells using Liberase^{TM} TL (research grade, Roche) for 12 minutes at 37°C. Single cell samples were immediately transferred to the University of Michigan Advanced Genomics Core facility for further processing. Further details were previously published[S13] and available at KPMP.org.

Urine cell preparation for scRNAseq in patients with COVID-19

Urine single cell preparation followed the protocol by Arazi et al.[S14] with various modifications. Briefly, COV urine was filtered through a 30 µm strainer into 50 ml tubes and centrifuged at 200 x *g* at 4°C for 10 minutes. After removing and storing the supernatant the cell pellet was washed once with 1 ml cold X-VIVO™10 medium (Cat#: 04-743Q, Lonza) and centrifuged in 1.5 ml tubes for 5 minutes at 200 x *g* at 4°C. The resulting cell pellet was then suspended in 50 µl DMEM/F12 medium supplemented with HEPES and 10% (v/v) FBS and about 50,000 cells were loaded onto the single cell droplet-based RNAseq platform. Next generation sequencing was carried out on a NovaSeq6000 (Illumina) machine generating a 200 million read depth per sample. All procedures were performed following biosafety precautions as directed by the Centers for Disease Control and Prevention and the University of Michigan guidelines.

scRNAseq data generation and analysis

ScRNAseq data generation followed methods developed for the Kidney Precision Medicine Project (KPMP) and are described in detail in supplement and at KPMP.org. In brief, individual cell barcoding, reverse RNA transcription, library generation and single cell sequencing using Illumina were all performed using the 10X Genomics protocol[S13]. The output from the sequencer was first processed by CellRanger, the proprietary 10X Chromium single cell gene expression analysis software (https://support.10xgenomics.com/single-cell-gene-expression/software/pipelines/latest/what-is-cell-ranger). Data analyses were performed on the CellRanger output data files using the Seurat 3 R package (https://cran.r-project.org/web/packages/Seurat/index.html). As a quality control step, cells with less than 500 or greater than 5000 genes per cell were filtered out, with the lower cut off as a threshold for cell viability and the higher cut off to remove cell duplets. This study used a cutoff of <50% mitochondrial reads per cell as an additional threshold for cell viability. A combined analysis of

the single cell datasets generated from the different sample sources (LD and DKD) was performed using Seurat (v3) that included the following steps: default normalization, scaling based on sample mRNA count and mitochondrial RNA content, dimensionality reduction PCA (Principal component analysis) and UMAP (Uniform Manifold Approximation and Projection), sample integration using Harmony algorithm, standard unsupervised clustering, and the discovery of differentially expressed cell type specific markers[S15]. According to Seurat, the normalization step uses a global-scaling method that normalizes the gene expression measurement for each cell by the total expression, multiplies this by 10,000 (default) and log-transforms the scaled expression values. For cell type annotation we used publicly available resources including published literature, Kidney Interactive Transcriptome (http://humphreyslab.com/SingleCell/), Human Protein Atlas (HPA) (https://www.proteinatlas.org), the Epithelial Systems Biology Laboratory (ESBL) (https://hpcwebapps.cit.nih.gov/ESBL/Database/), scRNAseq data and Immgen (https://www.immgen.org/). The same analysis processes were used for the COV samples except that no Harmony-based integration step was performed.

Further functional analyses were focused on PTEC expressing detectable ACE2 (ACE2+) and without ACE2 (ACE2-) mRNA in the different samples studied. In order to identify PTEC, for the DKD analysis, we filtered for cells in the PTEC and DTL/PTEC clusters with CUBN expression, and for COV clusters with CUBN, GATM, or LRP2 expression[S13, S16].

In situ hybridization of ACE2 in control and diabetic kidney biopsies

In situ detection of ACE2 (RNAscope® Probe Hs-ACE2, Advanced Cell Diagnostics [ACD], catalog #848151), mRNA transcripts using the RNAscope kit (ACD) was performed according to the manufacturer's protocol by kidney pathologists able to identify cell types in kidney tissue. Sections (3 μm) sections of de-identified human kidney tissue were cut from formalin-fixed, paraffin-embedded (FFPE) blocks supplied by the University of Michigan Tissue Procurement

Service. Housekeeping gene ubiquitin C (UBC, RNAscope® Positive Control Probe Hs-UBC, ACD, Catalog #310041) was used as an internal mRNA control and the bacteria DapB (RNAscope® Negative Control Probe- DapB, ACD, Catalog #310043) as a negative control gene. A horseradish peroxidase–based signal amplification system (RNAscope 2.0 HD Detection Kit-Brown, ACD, catalog 310035) was used for hybridization to the target probes, followed by color development with DAB, and the slides were counter-stained with hematoxylin (RICCA Chemical Company, catalog 3535-16). Positive staining was determined by brown punctate dots in the cytoplasm.

Functional network analysis

To determine the biological processes and pathways in the ACE2+ differentially expressed gene sets, we performed functional network clustering in the PTEC gene functional network derived from GIANT 2.0[S17, S18]. This network was generated through regularized Bayesian integration of 61,400 publicly available expression, physical interaction and other omics experiments to generate a fully connected weighted graph representing functional relationships in biological pathways in PTEC. Community clustering in the network was performed to identify tightly connected sets of genes using HumanBase.io module detection function[S19] (hb.flatironinstitute.org/covid-kidney). The network was clustered with each set of differentially expressed genes constituting each ACE2+ signature: LD, DKD, DKD-induced, and COV (Supplementary Table 1-3, 10). Specifically, for DKD and DKD-induced signatures, we clustered genes with Bonferroni adjusted p-value < 0.05, positive log fold-change, and found in at least 10% of cells. In order to cluster gene sets of similar sizes we limited the DKD signature (with a total size of 3735 genes) to the top 3000 genes by p-value significance for clustering. Due to the comparatively small number of PTEC in COV samples, ACE2+ co-regulated genes that passed a nominal uncorrected p-value threshold of 0.05, positive log fold-change, and were found in at least 10% of cells were selected. (2896 genes were clustered in the network). The Gene

Ontology enrichment outputs are Supplementary Tables 4,5,11,13,15,16 and can

be interactively explored at hb.flatironinstitute.org/covid-kidney.

Supplementary References:

S1. Bojkova D, Westhaus S, Costa R*, et al.* Sofosbuvir Activates EGFR-Dependent Pathways in Hepatoma Cells with Implications for Liver-Related Pathological Processes. *Cells* 2020; **9**.

S2. Klein S, Cortese M, Winter SL*, et al.* SARS-CoV-2 structure and replication characterized by in situ cryo-electron tomography. *bioRxiv* 2020**:** 2020.2006.2023.167064.

S3. Ng DK, Robertson CC, Woroniecki RP*, et al.* APOL1-associated glomerular disease among African-American children: a collaboration of the Chronic Kidney Disease in Children (CKiD) and Nephrotic Syndrome Study Network (NEPTUNE) cohorts. *Nephrol Dial Transplant* 2017; **32:** 983-990.

S4. Siu KL, Kok KH, Ng MH*, et al.* Severe acute respiratory syndrome coronavirus M protein inhibits type I interferon production by impeding the formation of TRAF3.TANK.TBK1/IKKepsilon complex. *J Biol Chem* 2009; **284:** 16202-16209.

S5. Liao M, Liu Y, Yuan J*, et al.* The landscape of lung bronchoalveolar immune cells in COVID-19 revealed by single-cell RNA sequencing. *medRxiv* 2020**:** 2020.2002.2023.20026690.

S6. Le Sage V, Cinti A, Amorim R*, et al.* Adapting the Stress Response: Viral Subversion of the mTOR Signaling Pathway. *Viruses* 2016; **8:** 152.

S7. Siu K-L, Yuen K-S, Castaño-Rodriguez C*, et al.* Severe acute respiratory syndrome coronavirus ORF3a protein activates the NLRP3 inflammasome by promoting TRAF3-dependent ubiquitination of ASC. *The FASEB Journal* 2019; **33:** 8865-8877.

S8. Cottam EM, Whelband MC, Wileman T. Coronavirus NSP6 restricts autophagosome expansion. *Autophagy* 2014; **10:** 1426-1441.

S9. Harder JL, Menon R, Otto EA*, et al.* Organoid single cell profiling identifies a transcriptional signature of glomerular disease. *JCI Insight* 2019; **4**.

S10. Monteil V, Kwon H, Prado P*, et al.* Inhibition of SARS-CoV-2 Infections in Engineered Human Tissues Using Clinical-Grade Soluble Human ACE2. *Cell* 2020.

S11. Looker HC, Mauer M, Saulnier P-J*, et al.* Changes in Albuminuria But Not GFR are Associated with Early Changes in Kidney Structure in Type 2 Diabetes. *J Am Soc Nephrol* 2019; **30:** 1049-1059.

S12. Delanaye P, Radermecker RP, Rorive M*, et al.* Indexing glomerular filtration rate for body surface area in obese patients is misleading: concept and example. *Nephrology Dialysis Transplantation* 2005; **20:** 2024-2028.

S13. Menon R, Otto EA, Hoover P*, et al.* Single cell transcriptomics identifies focal segmental glomerulosclerosis remission endothelial biomarker. *JCI Insight* 2020; **5**.

S14. Arazi A, Rao DA, Berthier CC*, et al.* The immune cell landscape in kidneys of patients with lupus nephritis. *Nat Immunol* 2019; **20:** 902-914.

S15. Stuart T, Butler A, Hoffman P*, et al.* Comprehensive Integration of Single-Cell Data. *Cell* 2019; **177:** 1888-1902.e1821.

S16. Wu H, Malone AF, Donnelly EL*, et al.* Single-Cell Transcriptomics of a Human Kidney Allograft Biopsy Specimen Defines a Diverse Inflammatory Response. *J Am Soc Nephrol* 2018; **29:** 2069-2080.

S17. Wong AK, Krishnan A, Troyanskaya OG. GIANT 2.0: genome-scale integrated analysis of gene networks in tissues. *Nucleic Acids Res* 2018; **46:** W65-W70.

S18. Greene CS, Krishnan A, Wong AK*, et al.* Understanding multicellular function and disease with human tissue-specific networks. *Nat Genet* 2015; **47:** 569-576.

S19. Krishnan A, Zhang R, Yao V*, et al.* Genome-wide prediction and functional characterization of the genetic basis of autism spectrum disorder. *Nat Neurosci* 2016; **19:** 1454-1462.

Supplementary Figure 1: UMAP plot showing the distribution of the cells in the 21 clusters resulting from the unsupervised clustering of the scRNA-seq data from DKD (red) and LD biopsies (blue).

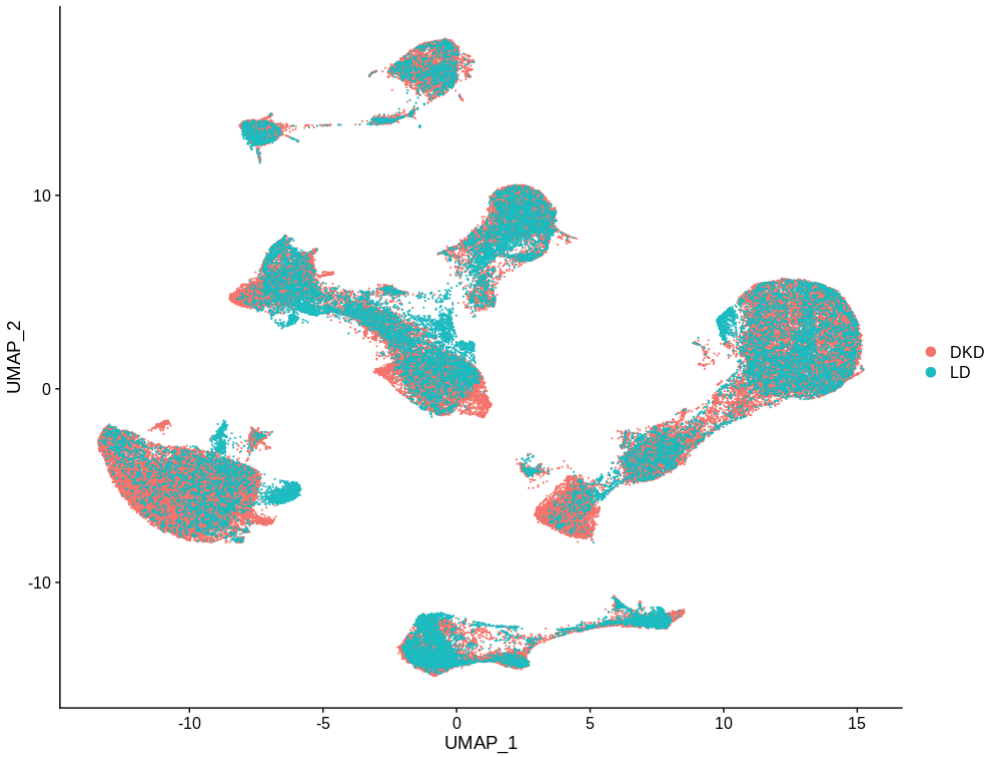

Supplementary Figure 2: Functional summary of DKD-induced ACE2+ expression signature. (A) The DKD-induced ACE2+ signature was used for community clustering in a PTEC-specific functional network to identify enriched processes and pathways. DKD-induced genes are significantly upregulated in DKD ACE2+ cells compared to LD ACE2+ cells, representing a signature pinpointing unique molecular features of the DKD ACE2-expressing cells. (B) Highlight of DKD-induced ACE2+ signature genes (red circles) shared with the set of proteins that increase expression in response to SARS-CoV-2 infection (Bojkova proteome* , Supplementary Table 6). Red text indicates modules with the strongest overlap ($p < 0.05$), thus highlighting modules and processes in the ACE2+ signature relevant to SARS-CoV-2 infection.

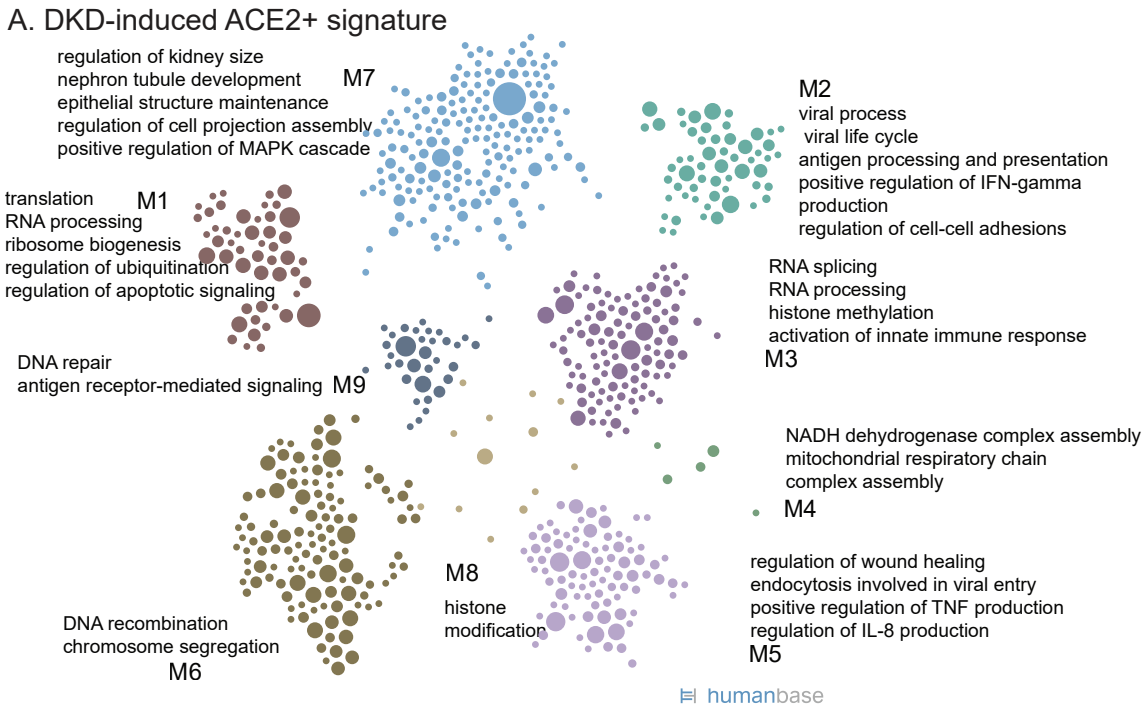

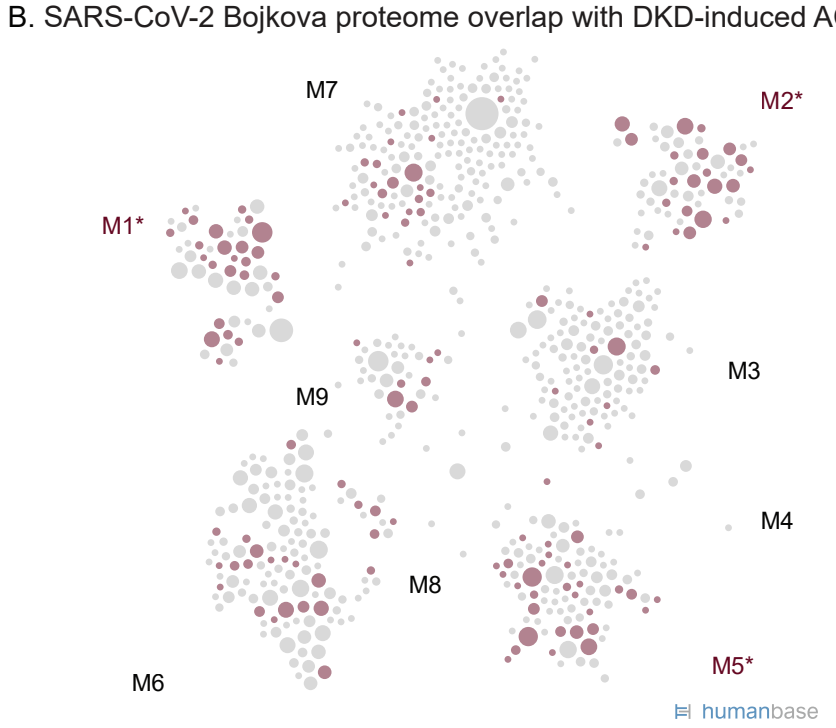

*Bojkova D, Westhaus S, Costa R, et al. Cells 2020; 9.

Supplementary Figure 3: Heatmap of cluster markers used to identify cell types in COV

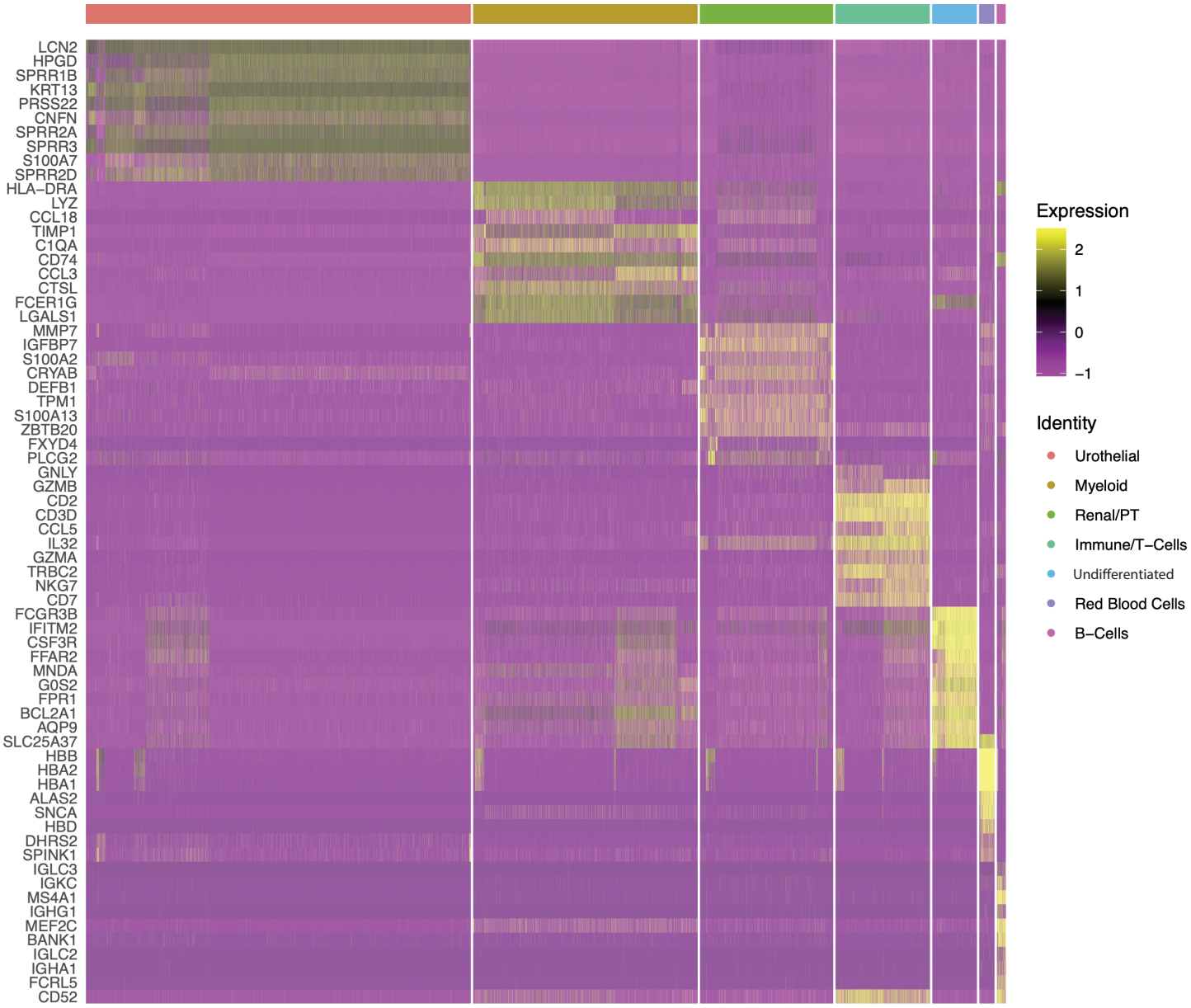

Supplementary Figure 4: ACE2 protein distribution in human kidney tissue

Figure obtained through the human protein atlas (accessed on 05/6/2020 from proteinatlas.org) of ACE2 expression in a normal kidney tissue sample shows predominant proximal tubular epithelial immunohistochemical staining by the ACE2 antibody.